Available online at www.sciencedirect.com

ScienceDirect

Geochimica et Cosmochimica Acta 211 (2017) 48–63

Geochimica et Cosmochimica Acta

www.elsevier.com/locate/gca

Copper isotope fractionation during partial melting and melt percolation in the upper mantle: Evidence from massif peridotites in Ivrea-Verbano Zone, Italian Alps

Jian Huang [a,*], Fang Huang [a,*], Zaicong Wang [b], Xingchao Zhang [a], Huimin Yu [a]

[a] CAS Key Laboratory of Crust-Mantle Materials and Environments, School of Earth and Space Sciences, University of Science and Technology of China, Hefei 230026, China

[b] Freie Universität Berlin, Institut für Geologische Wissenschaften, Malteserstrasse 74-100, 12249 Berlin, Germany

Received 12 October 2016; accepted in revised form 4 May 2017; Available online 11 May 2017

Abstract

To investigate the behavior of Cu isotopes during partial melting and melt percolation in the mantle, we have analyzed Cu isotopic compositions of a suite of well-characterized Paleozoic peridotites from the Balmuccia and Baldissero massifs in the Ivrea-Verbano Zone (IVZ, Northern Italy). Our results show that fresh lherzolites and harzburgites have a large variation of δ^{65}Cu ranging from −0.133 to 0.379‰, which are negatively correlated with Al_2O_3 contents as well as incompatible platinum-group (e.g., Pd) and chalcophile element (e.g., Cu, S, Se, and Te) contents. The high δ^{65}Cu can be explained by Cu isotope fractionation during partial melting of a sulfide-bearing peridotite source, with the light isotope (^{63}Cu) preferentially entering the melts. The low δ^{65}Cu can be attributed to precipitation of sulfides enriched in ^{63}Cu during sulfur-saturated melt percolation. Replacive dunites from the Balmuccia massif display high δ^{65}Cu from 0.544 to 0.610‰ with lower Re, Pd, S, Se, and Te contents and lower Pd/Ir ratios relative to lherzolites, which may result from dissolution of sulfides during interactions between S-undersaturated melts and lherzolites at high melt/rock ratios. Thus, our results suggest that partial melting and melt percolation largely account for the Cu isotopic heterogeneity of the upper mantle.

The correlation between δ^{65}Cu and Cu contents of the lherzolites and harzburgites was used to model Cu isotope fractionation during partial melting of a sulfide-bearing peridotite, because Cu is predominantly hosted in sulfide. The modelling results indicate an isotope fractionation factor of $\alpha_{\text{melt-peridotite}} = 0.99980–0.99965$ (i.e., $10^3\ln\alpha_{\text{melt-peridotite}} = -0.20$ to −0.35‰). In order to explain the Cu isotopic systematics of komatiites and mid-ocean ridge basalts reported previously, the estimated $\alpha_{\text{melt-peridotite}}$ was used to simulate Cu isotopic variations in melts generated by variable degrees of mantle melting. The results suggest that high degrees (>25%) of partial melting extracts nearly all source Cu and it cannot produce Cu isotope fractionation in komatiites relative to their mantle source, and that sulfide segregation during magma evolution have modified Cu isotopic compositions of mid-ocean ridge basalts.

Keywords: Cu isotope fractionation; Massif peridotite; Mantle melting; Melt percolation; Upper mantle

1. INTRODUCTION

Copper (Cu) is a moderately volatile, chalcophile, redox-sensitive (Cu^+ and Cu^{2+}) transition metal element. It has two stable isotopes of ^{65}Cu (69.17%) and ^{63}Cu (30.83%) (Shields et al., 1964), which can be significantly fractionated

* Corresponding authors.
E-mail addresses: jianhuang@ustc.edu.cn (J. Huang), fhuang@ustc.edu.cn (F. Huang).

http://dx.doi.org/10.1016/j.gca.2017.05.007
0016-7037/

during both low and high temperature geochemical processes (e.g., Albarède, 2004; Moynier et al., 2017). Due to the recent advance of high-precision isotope analytical method using multi-collector inductively coupled plasma mass spectrometry (MC-ICPMS), Cu isotopes have been used to unravel a number of fundamental issues such as the evolution of early solar system (e.g., Luck et al., 2005), core-mantle differentiation (Savage et al., 2015), continental weathering (e.g., Mathur et al., 2012), biological and hydrothermal activities (e.g., Mathur et al., 2005, 2010), sources of Cu in porphyry deposits (e.g., Mathur et al., 2009; Li et al., 2010), and source heterogeneity of granitic rocks (Li et al., 2009).

Recent studies have revealed that the Earth's mantle has highly variable Cu isotopic compositions with $\delta^{65}Cu$ ($= [(^{65}Cu/^{63}Cu)_{sample}/(^{65}Cu/^{63}Cu)_{NIST976} - 1] \times 1000‰$) ranging from −0.68 to 1.82‰ (Savage et al., 2014; Liu et al., 2015). Such Cu isotopic heterogeneity has been interpreted to result from recycling of crustal materials into the mantle (Savage et al., 2014; Liu et al., 2015). However, Liu et al. (2015) showed that peridotites devoid of modification by recycled crustal materials also display significant Cu isotopic variations with $\delta^{65}Cu$ ranging from −0.24 to 0.19‰. This suggests that other unidentified processes had altered the Cu isotopic compositions of mantle peridotites. In addition to crustal recycling, mantle processes (e.g., partial melting and melt percolation) can also cause elemental and isotopic heterogeneity of the upper mantle (Bodinier and Godard, 2014 and references therein). Thus, understanding the behavior of Cu isotope fractionation during mantle processes is a prerequisite for better application of Cu isotopes in tracing the recycled crustal materials.

In situ analyses of minerals in mantle peridotites have clearly unraveled that sulfides usually have variably higher Cu contents (percent levels, e.g., 0.01–76.8 wt.%) relative to the coexisting silicate and oxide minerals such as olivine, pyroxene, garnet, and spinel (<5 ppm) (Garuti et al., 1984; Lorand, 1989; Luguet et al., 2001, 2003, 2004; Wang et al., 2009; Harvey et al., 2011; Lee et al., 2012). This is consistent with experimental results that sulfide has very high sulfide melt/silicate melt partition coefficients ($^{sulfide/melt}D_{Cu}$) of 600–1800 at upper mantle conditions (e.g., Gaetani and Grove, 1997; Ripley et al., 2002; Mungall and Brenan, 2014). Thus, sulfide is thought to be a dominant host of Cu in mantle peridotites (e.g., Lee et al., 2012; Wang and Becker, 2015a).

The primitive upper mantle has ~200 ppm sulfur (S) (Palme and O'Neill, 2014), and sulfide is ubiquitous in the upper mantle and generally involved in mantle melting and melt percolation (e.g., Garuti et al., 1984; Harvey et al., 2011; Lee et al., 2012; Wang et al., 2013; Le Roux et al., 2015). At equilibrium conditions, sulfide is enriched in the lighter Cu isotope (^{63}Cu) relative to the coexisting silicates as revealed by experimental studies (Savage et al., 2015) and studies on natural igneous systems (Huang et al., 2016a). It is also demonstrated that crystallization of silicate minerals does not significantly fractionate Cu isotopes, as attested to by Cu isotope measurements of differentiated cogenetic magmatic suites (Li et al., 2009; Huang et al., 2016a). These results imply that Cu isotopes can be potentially fractionated during melting of sulfide and melt percolation. For example, Savage et al. (2014) suggested that partial melting can fractionate Cu isotopes as they noted that the elementally depleted peridotite xenoliths from Kilbourne Hole have low $\delta^{65}Cu$ (down to −0.40‰). However, Liu et al. (2015) proposed that there is no detectable Cu isotope fractionation during mantle melting based on the similar Cu isotopic compositions between mantle peridotites devoid of metasomatism ($\delta^{65}Cu = -0.24$ to 0.19‰) and mantle-derived magmas, including mid-ocean ridge basalts (MORBs) and ocean island basalts (OIBs) ($\delta^{65}Cu = -0.07$ to 0.18‰). It is thus necessary to investigate the behavior of Cu isotopes during mantle melting to clarify such a debate.

In addition to partial melting, melt percolation influences the chemical evolution of the mantle (Bodinier and Godard, 2014 and references therein). The large variations of $\delta^{56}Fe$ (~1.5‰) (e.g., Weyer and Ionov, 2007; Zhao et al., 2015) and $\delta^{26}Mg$ (~0.6‰) (e.g., Xiao et al., 2013) in mantle peridotites result from both equilibrium and kinetic isotope fractionations during percolation of Fe-rich and Mg-poor silicate melts. The magnitude of kinetic isotope fractionation during melt percolation depends on differential diffusivities of isotopes and could be much larger than that observed in equilibrium processes at high temperatures (Sossi et al., 2016a and references therein). Previous studies have shown that S-saturated melt (i.e., sulfide melt) percolation with low melt/rock ratios would result in precipitation of interstitial sulfide with pyroxene and spinel (e.g., Lorand and Alard, 2001), whereas percolation of S-undersaturated silicate melts with high melt/rock ratios would dissolve these minerals and precipitate olivine (e.g., Kelemen et al., 1995). Accordingly, percolation by melts can redistribute platinum-group elements (PGEs, i.e., Os, Ir, Ru, Rh, Pt, and Pd) and chalcophile elements (e.g., Cu, S, Se, and Te) (e.g., Lorand and Alard, 2001; Wang et al., 2013; Wang and Becker, 2015a; Sanfilippo et al., 2016). However, the behavior of Cu isotopes during melt percolation involving dissolution and precipitation of sulfide remains unknown.

Here, we have determined the Cu isotopic compositions of a suite of well-characterized samples from the Baldissero (BD) and Balmuccia (BM) peridotite massifs in the Ivrea-Verbano Zone (IVZ, Italian Alps). Both peridotite massifs represent fragments of subcontinental lithosphere mantle (SCLM) and had been tectonically emplaced at the lower crustal level during the Alpine orogeny ca. 110 Ma ago (e.g., Quick et al., 2009). In contrast to xenolith peridotites which may experience interactions with the host lavas, massif peridotites are not subject to such interactions. Furthermore, their exposed areas (several km^2) allow an in-situ observation of mantle processes. The BD and BM peridotites are extremely fresh with no or limited modification (if any) by crustal materials (Hartmann and Hans Wedepohl, 1993; Rivalenti et al., 1995; Mazzucchelli et al., 2009, 2010). They are predominantly lherzolitic bodies with a small (10–15% by volume) fraction of harzburgites, dunites and pyroxenite veins (Shervais and Mukasa, 1991) and are modified by partial melting and percolation of melts with different compositions (Wang et al., 2013).

Therefore, they provide a great opportunity to examine the behavior of Cu isotopes during partial melting and melt percolation in the upper mantle. Our results reveal a δ^{65}Cu range from −0.133 to 0.379‰ for the fresh lherzolites and harzburgites and from 0.544 to 0.610‰ for the BM dunites. The high δ^{65}Cu was caused by partial melting and S-undersaturated melt percolation with preferential dissolution of sulfide enriched in the light Cu isotope, whereas the low δ^{65}Cu was caused by sulfide melt percolation. Our observations suggest that partial melting and melt percolation likely result in significant Cu isotopic heterogeneity of the upper mantle and that partial melting and/or sulfide segregation during magma differentiation control the Cu isotopic compositions of komatiites and MORBs.

2. GEOLOGICAL SETTINGS AND SAMPLE DESCRIPTIONS

The IVZ in the Western Italian Alps represents one of the best preserved cross-sections of the lower continental crust. It was formed by the Alpine collision between the Adriatic and Europe Plates (e.g., Quick et al., 2009) and comprises two main units of the Kinzigite Formation and the Mafic Complex with the later intruding into the former over a protracted time interval between 290 Ma and 210 Ma (Peressini et al., 2007) (Fig. 1).

The BM peridotite massif is a tectonic lens of 4.5 km long and 0.8 km wide within the mafic-ultramafic complex (Fig. 1). It predominantly consists of spinel lherzolite (>85% by volume), subordinate dunite (~10%), and rare harzburgite (Shervais and Mukasa, 1991; Mukasa and Shervais, 1999). The chemical compositions of the BM lherzolite record low degrees of melt extraction and nearly simultaneous melt infiltration during the late Paleozoic (Rivalenti et al., 1995; Mukasa and Shervais, 1999; Mazzucchelli et al., 2009; Wang et al., 2013). The spinel lherzolite is cut by two main generations of pyroxenite dykes, including the older Cr-diopside websterites and the younger Al-augite clinopyroxenites (Shervais and Mukasa, 1991; Wang and Becker, 2015b). These dykes reflect multistage events of melt intrusion before the emplacement of the BM massif into the lower crust

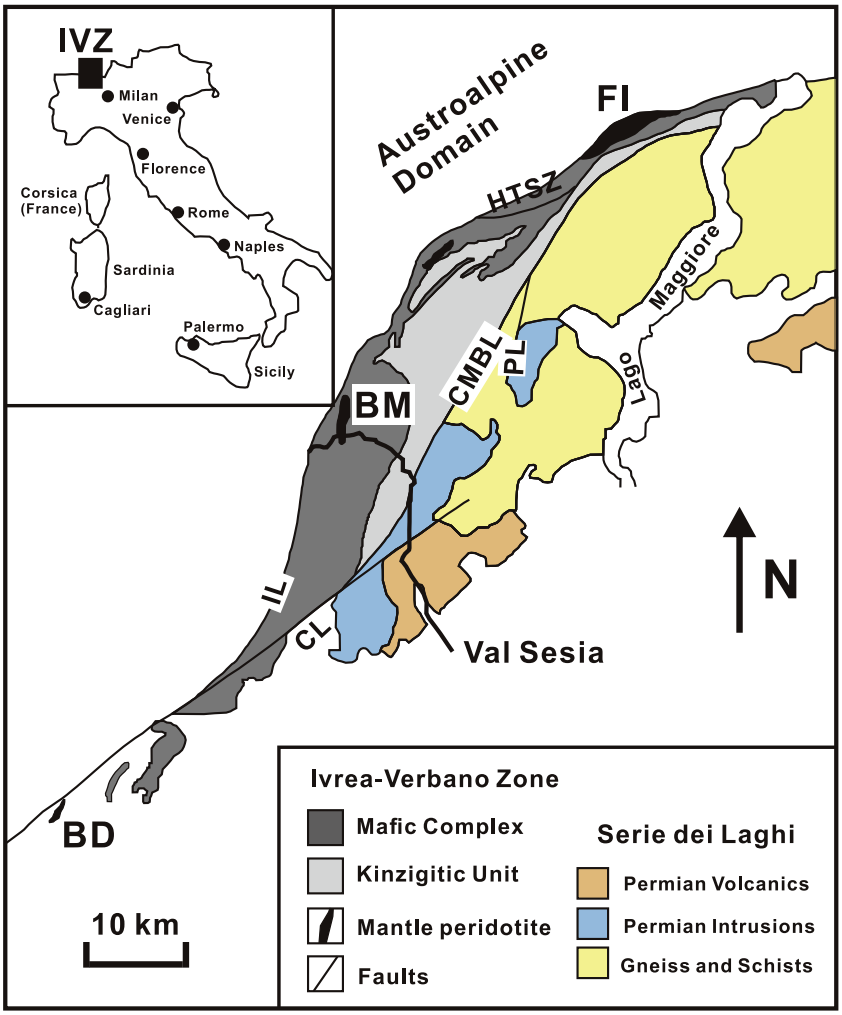

Fig. 1. Geological map of the Ivrea-Verbano Zone with locations of the Baldissero (BD) and Balmuccia (BM) peridotite massifs (Modified after Mazzucchelli et al., 2010). FI = Finero; CL = Cremoina line; IL = Insubric line; CMBL = Cossato-Mergozzo-Brissago line; PL = Pogallo line; HTSZ = High-temperature shear zone.

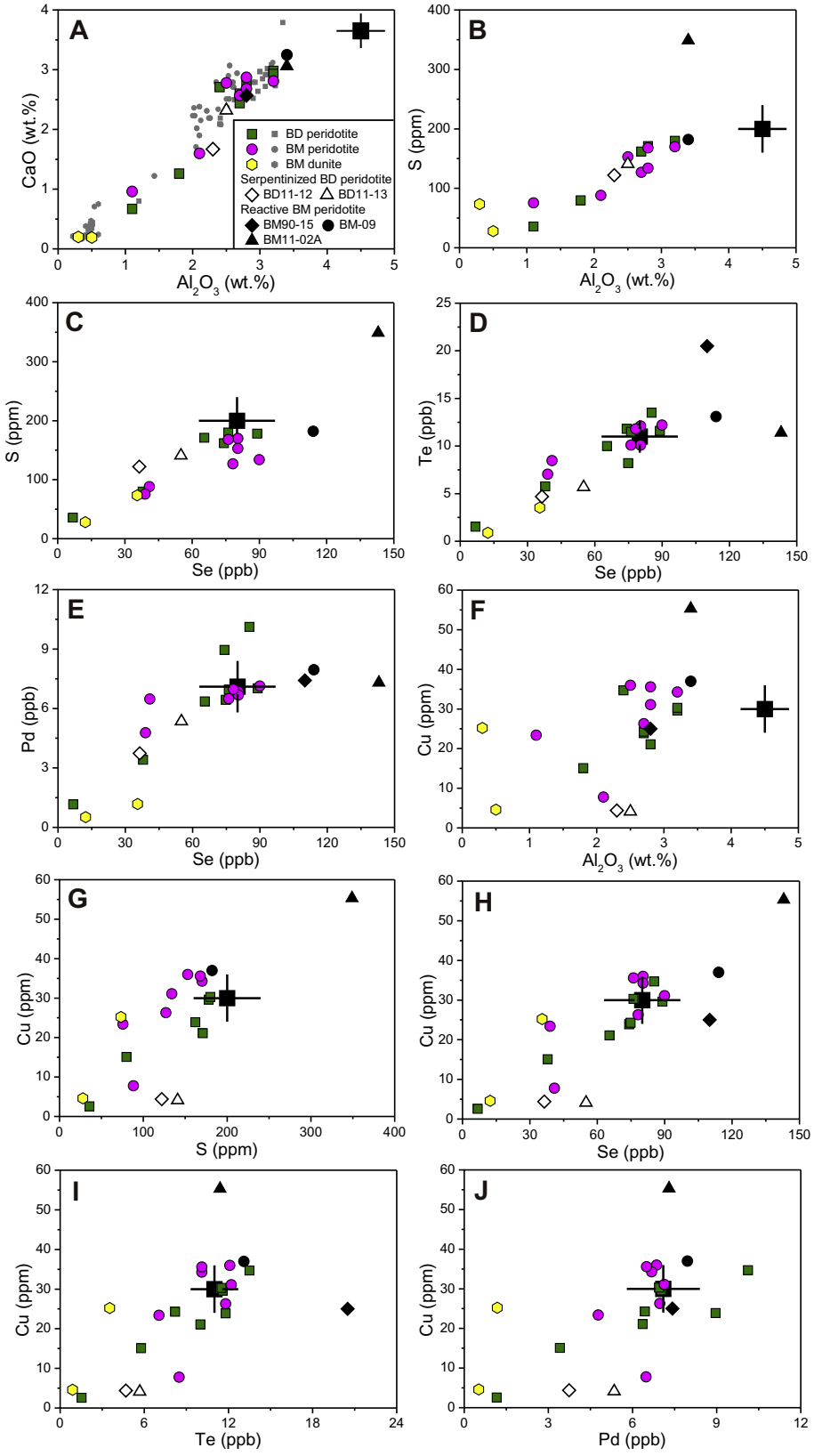

Fig. 2. Variations of selected element contents in Baldissero and Balmuccia peridotites. CaO and Al_2O_3 data in (A) are from previous studies (Hartmann and Hans Wedepohl, 1993; Obermiller, 1994; Rivalenti et al., 1995; Mazzucchelli et al., 2009, 2010; Wang et al., 2013), and trace element data are from Wang et al. (2013). Colored and specifically-denoted symbols denote the samples investigated in this study. Black squares denote the primitive mantle (Becker et al., 2006; Wang and Becker, 2013, 2015a; Palme and O'Neill, 2014). (For interpretation of the references to colour in this figure legend, the reader is referred to the web version of this article.)

(Rivalenti et al., 1995; Mukasa and Shervais, 1999). Elemental and Nd-Sr isotopic variations of the pyroxenite dykes have been considered as a response to thinning and uplift of the SCLM and upwelling of asthenosphere to the crustal level (Mukasa and Shervais, 1999). There are two main types of replacive dunites in the BM massif, including thin dunite layers (<40 cm thick) and tabular dunite bodies (50 m thick and 150 m long). They have been interpreted to originate from pyroxene- and sulfide-dissolving reactions caused by focused percolation of S-undersaturated silicate melts (Rivalenti et al., 1995; Mazzucchelli et al., 2009; Wang et al., 2013).

The BD massif is in the south-western part of the IVZ (Fig. 1). It is mainly composed of spinel lherzolites containing small amounts of amphibole and sulfide (e.g., Mazzucchelli et al., 2010). The BD lherzolite has the same major and trace element composition as that at Balmuccia (Hartmann and Hans Wedepohl, 1993). Incompatible element concentrations of whole rock and clinopyroxene suggest that the BD spinel lherzolite is a refractory residue after melt extraction (Mazzucchelli et al., 2010). Predominantly Paleozoic Re depletion ages (T_{RD}) and a Sm-Nd errorchron age (378 ± 48 Ma) of clinopyroxene separates from the BD spinel lherzolite record a Paleozoic partial melting event during the Variscan orogeny (Obermiller, 1994; Mazzucchelli et al., 2010; Wang et al., 2013). The BD massif is also cut by different generations of Mesozoic pyroxenite dykes (i.e., Cr-diopside and Al-augite suites) (Mazzucchelli et al., 2010). Notably, even some BD lherzolites far away from pyroxenite dykes may have been slightly affected by melt percolation, as revealed by the presence of accessory titanian pargasite and a slight enrichment of highly incompatible elements (e.g., Nb) in the bulk rock compositions (Mazzucchelli et al., 2010).

The BD and BM peridotites investigated here have been well studied previously for petrology and major/trace elemental and Sr-Nd-O-Os isotopic compositions (Obermiller, 1994; Rivalenti et al., 1995; Wang et al., 2013). They include 17 lherzolites, 3 harzburgites, and 2 tabular dunites, which represent the entire range of variations of bulk rock compositions reported in previous studies (Fig. 2A). All but two selected samples are exceptionally fresh, as indicated by the absence of altered minerals (e.g., serpentine) and low loss on ignition (LOI, typically <1 wt.% and sometimes negative) (Obermiller, 1994; Wang et al., 2013). Accordingly, sulfides in these samples are unaffected by alteration processes after emplacement. The major metal sulfides are pentlandite and subordinate chalcopyrite (>95% by volume) as interstitial and inclusion phases (Wang et al., 2013). The co-variations of Al_2O_3 and CaO contents (Fig. 2A) suggest that the studied peridotites have a variable fertility. Good correlations of S with Al_2O_3 and Se, Se with Te and Pd as well as Cu with Al_2O_3, Pd, S, Se, and Te can be observed in the studied samples (Fig. 2B–J).

3. ANALYTICAL METHODS

Copper isotopic analyses were performed at the Metal Stable Isotope Laboratory of the University of Science and Technology of China (USTC). The procedures for sample dissolution and chemical purification used here are modified from those established by Maréchal et al. (1999). Sample powders were dissolved in Savillex beakers with caps using double-distilled concentrated $HF + HNO_3$, $HCl + HNO_3$ and HCl successively. Separation of Cu was achieved by cation exchange chromatography with Bio-Rad AG-MP-1M strong anion resin in 6 N HCl + 0.001% H_2O_2 media. The column chemistry was performed twice, and then matrix elements of Na, Ti, Fe, Mg, and Al, which could have a significant impact on the analytical accuracy of Cu isotopes due to molecular spectral interference confirmed by our cation-doping experiments (Fig. S1), were checked for each eluted Cu fractions using ICP-MS. If matrix elements/Cu ratios (mass/mass) are high enough (i.e., Ti/Cu > 0.1, Na/Cu > 0.5, Fe/Cu > 2; Al/Cu > 2, Mg/Cu > 4) (Fig. S1) to affect the analytical accuracy, a further column chemistry was performed to ensure that these ratios are low enough to avoid a detectable molecular spectral interference. The Cu yields through column chemistry, obtained by analyses of Cu contents in the elution collected before and after the Cu cut, are >99.5%. The total procedural blanks (from sample dissolution to mass spectrometry) during the course of this study range from 0.81 to 2.34 ng ($n = 14$), which are negligible compared to ca.1.2 μg Cu loaded onto the resin.

Copper isotope ratios were analyzed by a sample-standard bracketing method using a Thermo-Fisher *Neptune Plus* MC-ICPMS. The low-mass-resolution mode and the SIS introduction system were applied with ^{63}Cu in the Central cup and ^{65}Cu in the H2 Faraday cup. A Ni (H) + Ni (Jet) cone was used with 150 ppb Cu yielding a ^{63}Cu signal of ca. 5.0 V. Copper isotope ratios are reported in standard δ-notation in per mil relative to NIST 976: $\delta^{65}Cu = [(^{65}Cu/^{63}Cu)_{sample}/(^{65}Cu/^{63}Cu)_{NIST\ 976} - 1] \times 1000‰$. Repeated analyses of two mono-element reference materials over one and a half years yield $\delta^{65}Cu$ of 0.192 ± 0.048‰ (2SD, $n = 347$) for ERM-AE-647 and 0.303 ± 0.049‰ (2SD, $n = 51$) for AAS (Fig. S2). Thus, the long-term external reproducibility for $\delta^{65}Cu$ is ±0.049‰ (2SD) during the course of this study. Seven international whole rock standards (i.e., AGV-2, BHVO-2, BCR-2, BIR-1a, GSP-2, W-2a, and PCC-1) were processed through column chemistry together with samples of interest for accuracy check. Their Cu isotopic compositions obtained here agree with previously-published values within error (Table S1, Chapman et al., 2006; Li et al., 2009; Bigalke et al., 2010a,b, 2011; Moynier et al., 2010; Moeller et al., 2012; Dekov et al., 2013; Liu et al., 2014a,b; Savage et al., 2015; Sossi et al., 2015; Huang et al., 2016a,b). This, combined with the indistinguishable results for repeated analyses (Table 1), assures the accuracy of our data.

4. RESULTS

The Cu isotopic compositions and selected previously-published major and trace element concentrations of the peridotites investigated here are listed in Table 1. The whole range of $\delta^{65}Cu$ varies from −0.344‰ to 0.610‰. Two dunites from the tabular dunite body at the BM massif show heavy Cu isotopic compositions with $\delta^{65}Cu$ from

Table 1
Copper isotopic compositions and selected element concentrations of Baldissero and Balmuccia peridotites from Ivrea-Verano Zone, Italian Alps.

Sample	Rock[a] Type	$\delta^{65}Cu$[b] ‰	2SD[c]	N[d]	Al_2O_3[e] wt.%	CaO[e] wt.%	Cu[e] ppm	Pd[e] ppb	S[e] ppm	Se[e] ppb	Te[e] ppb	Se/Te[e]	Pd/Ir[e]	$^{187}Os/^{188}Os$[e]
Baldissero														
BD11-01	L	0.083	0.044	3	2.7	2.44	23.9	8.96	162	74.2	11.8	6.3	2.29	0.12454
BD11-05	L	0.225	0.034	3	3.2	2.98	29.6	7.02	178	89.0	11.6	7.7	2.11	0.12935
BD11-07	L	0.073	0.042	3	2.8	2.78	21.1	6.36	171	65.4	10.0	6.5	1.82	0.12672
Replicate[f]		0.108	0.032	3										
Average[g]		0.090	0.049											
BD11-08	L	0.078	0.056	3	3.2	2.93	30.3	6.95	180	76.1	11.5	6.6	1.82	0.12770
BD11-12	L	0.256	0.054	3	2.3	1.67	4.39	3.74	122	36.4	4.69	7.8	1.32	0.12041
BD11-13	L	0.618	0.025	3	2.5	2.32	4.11	5.35	141	55.0	5.68	9.7	1.64	0.12223
Replicate		0.576	0.045	3										
Average		0.597	0.049											
BD90-4	L	−0.008	0.041	3	2.4	2.71	34.7	10.1		85.3	13.5	6.3	2.78	0.12613
BD90-10	L	0.239	0.024	3	2.7	2.60	24.3	6.44		74.8	8.20	9.1	1.56	0.12303
BD92-2	H	0.205	0.042	3	1.8	1.26	15.1	3.41	79.9	37.9	5.77	6.6	1.13	0.11986
BD-17	H	0.379	0.091	3	1.1	0.67	2.59	1.16	35.8	6.8	1.53	4.5	0.46	0.11776
Balmuccia														
BM90-15	L	−0.315	0.048	3		2.57	25.0	7.42		110	20.5	5.4	1.94	0.12578
Replicate		−0.373	0.034	3										
Average		−0.344	0.049		2.8									
BM-09	L	−0.007	0.026	3	3.4	3.25	37.0	7.96	182	114	13.1	8.7	2.01	0.13125
BM11-02A	L	−0.137	0.035	3	3.4	3.06	55.3	7.30	349	143	11.4	12.5	1.88	0.13167
Replicate		−0.128	0.010	3										
Average		−0.133	0.049											
BM11-03B	H	0.176	0.044	3	1.1	0.96	23.4	4.78	75.7	39.0	7.05	5.5	1.11	0.11914
BM11-04	L	0.084	0.018	3	2.5	2.78	36.0	6.86	153	80.4	12.1	6.6	1.78	0.12667
BM11-08	L	0.040	0.028	3	3.2	2.81	34.3	6.68	170	80.4	10.1	7.9	1.70	0.12734
BM11-09	L	0.092	0.013	3	2.7	2.57	26.3	6.97	127	78.2	11.8	6.6	1.78	0.12613
BM11-10	L	0.100	0.016	3	2.8	2.87	31.1	7.13	134	89.9	12.2	7.4	1.81	0.12702
BM11-11	L	0.250	0.035	3	2.1	1.60	7.80	6.48	88.1	40.9	8.48	4.8	1.62	0.12493
BM11-18	L	0.214	0.049	3	2.8	2.68	35.6	6.50	168	76.1	10.1	7.6	1.79	0.12649
BM11-07A	D	0.554	0.044	3	0.30	0.20	25.2	1.18	73.4	35.5	3.53	10.1	0.60	0.12625
Replicate		0.534	0.029	3										
Average		0.544	0.049											
BM11-24A	D	0.610	0.053	3	0.50	0.19	4.61	0.52	27.9	12.3	0.89	13.8	0.72	0.12946

[a] L = Lherzolite, H = Harzburgite, D = Dunite.
[b] $\delta^{65}Cu = [(^{65}Cu/^{63}Cu)_{sample}/(^{65}Cu/^{63}Cu)_{NIST\ 976} - 1] \times 1000$, where NIST 976 is an international Cu isotope-normalized standard.
[c] 2SD = two times the standard deviation of the population of n repeated measurements of the same solution.
[d] *N* represents the times of repeat measurements of the same purified solution by MC-ICP-MS.
[e] Data for Cu concentrations are taken from Wang and Becker (2015a,b), and the others from Wang et al. (2013).
[f] Repeated = repeated the whole procedure, including sample dissolution, column chemistry and mass spectrometry.
[g] The average values were used in all plots and discussion. For these values, the long-term reproducibility (0.049‰, 2SD) during the course of data acquirement is cited.

0.544‰ to 0.610‰ (Fig. 3). One spinel lherzolite (sample DB11-13) with serpentinization (Wang et al., 2013) have a $\delta^{65}Cu$ value of 0.597‰, whereas one spinel lherzolite (sample BM90-15) modified by a late-stage melt/fluid transport (Wang et al., 2013), has the lowest $\delta^{65}Cu$ of −0.344‰ (Fig. 3). With the exception of these four samples, $\delta^{65}Cu$ values of the rest eighteen peridotites display negative correlations with Al_2O_3, Cu, S, Se, Te, and Pd contents (Fig. 3).

5. DISCUSSION

Previous studies have revealed that fresh lherzolites and harzburgites from the BD and BM massifs are mantle residues after low to high degrees of melt extraction (Hartmann and Hans Wedepohl, 1993; Rivalenti et al., 1995; Mazzucchelli et al., 2010; Wang et al., 2013). This is evidenced by the good correlation between CaO and Al_2O_3 (Fig. 2A and B). Among 22 samples studied here, two lherzolites (samples BD11-12 and BD11-13) had experienced low temperature serpentinization (Wang et al., 2013). Three lherzolites (samples BM90-15, BM-09, and BM11-02A) have notably higher S, Se, Te and/or Cu contents relative to other peridotites and the primitive mantle (PM) (Fig. 2B–J), suggesting local sulfide melt percolation at the BM peridotite massif (Wang et al., 2013). Two replacive dunites from the BM massif have much lower contents of incompatible PGEs (e.g., Re, Pt, and Pd) and chalcophile elements (Fig. 2B–E), but variably higher contents of compatible PGEs (e.g., Ir, Ru, and Rh), higher S/Se and Se/Te

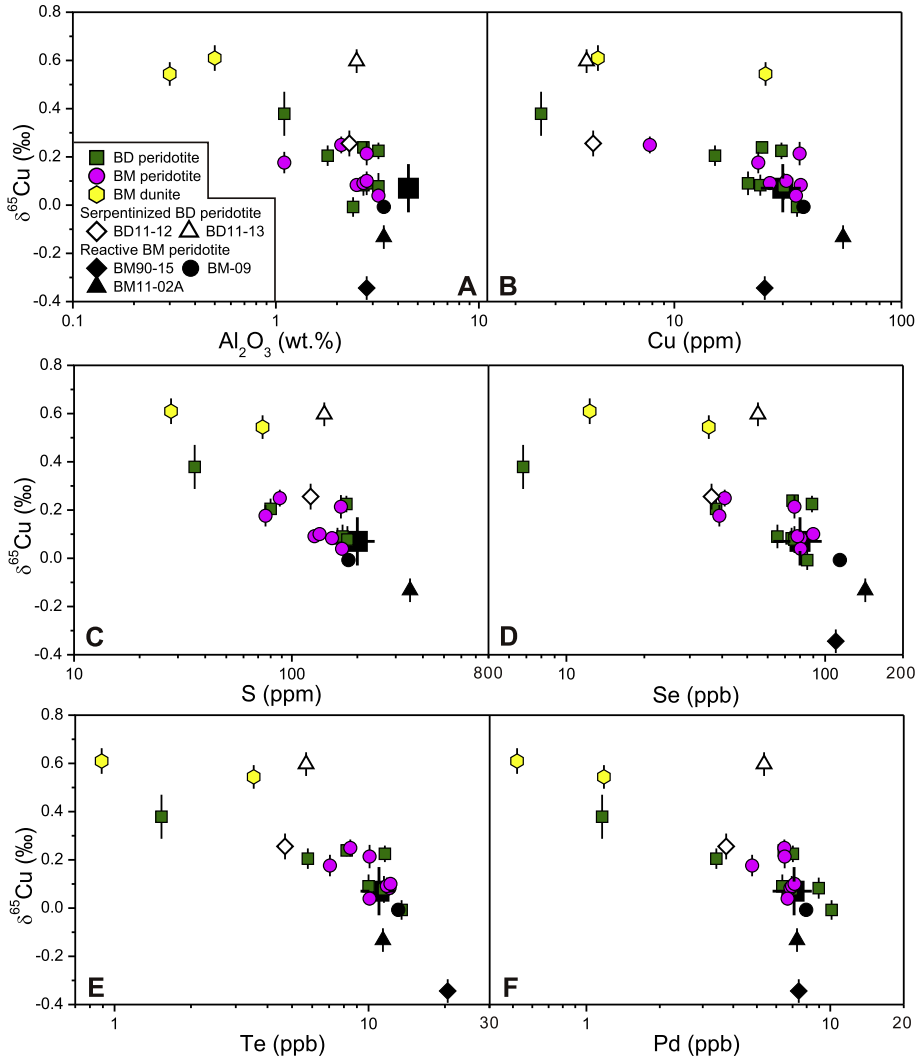

Fig. 3. $\delta^{65}Cu$ versus Al_2O_3 (A), Cu (B), S (C), Se (D), Te (E), and Pd (F) in Baldissero and Balmuccia peridotites. The *X*-axis is the logarithmic coordinate. The $\delta^{65}Cu$ of the primitive mantle (black squares) is from Savage et al. (2015), and data sources for element contents are the same as Fig. 2.

relative to the BM lherzolites (Wang et al., 2013). In addition, the BM dunites and lherzolites have similar $^{187}Os/^{188}Os$ (Fig. 4A, Wang et al., 2013). Such geochemical characteristics of dunites might result from S-undersaturated silicate melt-lherzolite interactions at high melt/rock ratios with preferential dissolution of sulfide (Wang et al., 2013). Below, we thus first discuss the behavior of Cu isotopes during low temperature serpentinization, partial melting, sulfide melt percolation, and S-undersaturated melt percolation, and then the implications of our observations for the Cu isotopic heterogeneity of the upper mantle and the Cu isotopic compositions of MORBs and komatiites.

5.1. Effects of low temperature alteration

Low-temperature alteration processes (such as weathering and serpentinization) can influence the Cu elemental and isotopic compositions in altered rocks and minerals (e.g., Mathur et al., 2005, 2012; Wang and Becker, 2015a). Most samples studied here are fresh as indicated by the absence of serpentine minerals, the lack of sulfide alteration, and low LOI (typically <1 wt.%) (Wang et al., 2013). The systematic variations of Cu and $\delta^{65}Cu$ with lithophile fertility indices (e.g., Al_2O_3) and alteration-sensitive chalcophile elements (e.g., S, Se, and Te) (Figs. 2F–I, 3) strongly suggest the negligible effect of low temperature alteration. This is further supported by the systematic variations of S, Se, and Te with each other and with Al_2O_3 and incompatible PGEs (e.g., Pd) (Fig. 2B–E). The exception is sample BD11-13 that displays much higher $\delta^{65}Cu$ (0.597‰) relative to other samples at given Al, Cu, S, Se, Te, and Pd contents (Fig. 3). Identification of serpentinized cracks and relatively high LOI (~2.5 wt.%) in this sample suggest that it had experienced low temperature alteration processes (Wang et al., 2013). Such processes had been invoked to explain the extremely low $\delta^{65}Cu$ (−0.67 to −0.41‰) of secondary native copper grains in a

plagioclase lherzolite from the Horoman peridotite massif (Ikehata and Hirata, 2012). Li et al. (2009) also suggested that such processes were responsible for the abnormally high δ^{65}Cu (up to 1.51‰) of two granites from the Lachlan Fold Belt in southeastern Australia. Thus, we suggest that localized secondary alteration processes could be reasons for the heavy Cu isotopic composition of sample BD11-13. Accordingly, this sample will not be taken into account in the following discussions.

5.2. Copper isotope fractionation during mantle melting

Variable partition coefficients of Cu between silicate minerals and melts ($^{\text{silicate mineral/melt}}D_{Cu}$) have led to different understanding of the significance of sulfides and silicates in controlling Cu partitioning during partial melting of peridotites (Fellows and Canil, 2012; Lee et al., 2012; Liu et al., 2014c). Experimentally determined $^{Ol/melt}D_{Cu}$ (about 0.05) are similar, but there exists a great difference in $^{Cpx/melt}D_{Cu}$ and $^{Opx/melt}D_{Cu}$ (Fellows and Canil, 2012; Liu et al., 2014c, both S-free experiments). Using Cu-free noble metal capsules (i.e., Re, Pt), Fellows and Canil (2012) obtained $^{Cpx/melt}D_{Cu}$ of 0.23 and $D_{Cu}^{Opx/melt}$ of 0.15, much higher than those ($^{Cpx/melt}D_{Cu} = 0.06$, $^{Opx/melt}D_{Cu} = 0.04$) determined using $Pt_{95}Cu_{0.5}$ alloy capsules (Liu et al., 2014c). $^{Ol/melt}D_{Cu}$, $^{Cpx/melt}D_{Cu}$, and $^{Opx/melt}D_{Cu}$ from Liu et al. (2014c) are similar to those estimated from in situ laser ablation ICP-MS analyses of natural minerals and groundmass in basalts (Lee et al., 2012). These results indicate only weak lithophile affinity of Cu in mantle peridotites.

Although silicate phases are likely to host a small fraction of Cu, several lines of evidence suggest that Cu is predominantly hosted by sulfides in mantle peridotites. As illustrated in Fig. S3, sulfides in mantle peridotites have 0.01–76.8 wt.% Cu contents (e.g., Garuti et al., 1984; Lorand, 1989; Luguet et al., 2001, 2003, 2004; Wang et al., 2009; Harvey et al., 2011; Lee et al., 2012), much higher than those of olivine, pyroxene, garnet, and spinel (<5 ppm, Lee et al., 2012). High T-P experiments have indicated very high $^{sulfide/melt}D_{Cu}$ of 600–1800 (e.g., Gaetani and Grove, 1997; Ripley et al., 2002; Mungall and Brenan, 2014), consistent with those estimated from in situ laser ablation ICP-MS analyses of sulfide droplets and glasses in MORBs (760–1600, Jenner et al., 2012; Patten et al., 2013). Even if the higher $^{Cpx/melt}D_{Cu}$ and $^{Opx/melt}D_{Cu}$ from Fellows and Canil (2012) were used, mass balance of sulfides and silicate phases and corresponding partition coefficients indicate that sulfide contribution accounts for >70% of the bulk rock D_{Cu} during low to moderate degrees of melting (Table S1). The sulfide contribution is even higher when the lower $^{Cpx/melt}D_{Cu}$ and $^{Opx/melt}D_{Cu}$ from Lee et al. (2012) and Liu et al. (2014c) are used for calculations (Table S2). As shown in Fig. 2F–I, the positive correlations of Cu with S, Se, and Te in the BD and BM peridotites are better than those with Al_2O_3, which is mainly hosted in pyroxene and spinel. Such features can be also observed in other orogenic peridotite massifs worldwide (Fig. S4). This also reflects the predominant chalcophile nature of Cu.

Mantle melting and melt extraction can cause significant Fe and Zn isotope fractionation (e.g., Weyer and Ionov, 2007; Doucet et al., 2016) but limited isotope fractionation of Li and Mg (e.g., Tomascak et al., 1999; An et al., 2017). Copper is a moderately incompatible element with $^{peridotite/melt}D_{Cu}$ of 0.49–0.60 in a sulfide-bearing peridotite system and $^{peridotite/melt}D_{Cu}$ of ca. 0.05 in a sulfide-absent peridotite system (Lee et al., 2012; Liu et al., 2014c; Le Roux et al., 2015). The presence of sulfide in the mantle source explains the higher Cu contents in oceanic and arc basalts (ca. 60–120 ppm) relative to the primitive mantle (30 ± 6 ppm) (Lee et al., 2012; Le Roux et al., 2015), consistent with the widespread existence of sulfide in orogenic and xenolith peridotites (e.g., Garuti et al., 1984; Luguet et al., 2001; Wang et al., 2013). The negative correlations of Cu and S with Al_2O_3 in the BD and BM peridotites (Fig. 2B and F) reflect extraction of melts enriched in Cu and S during partial melting. The good linear correlations of Cu with S, Se, Te, and Pd (Fig. 2G–J) strongly suggest that these elements behave similarly and Cu is dominantly controlled by sulfide during mantle melting. The δ^{65}Cu of peridotites show a negative correlation with the Al_2O_3 content (Fig. 3A), indicating a link between δ^{65}Cu and degrees of melt extraction. As Al_2O_3 contents of peridotites decrease with increasing degrees of partial melting (e.g., Walter, 1998), such a relationship further suggests that Cu isotopes are fractionated during partial melting with ^{63}Cu preferentially partitioning into the melts, leaving the residual peridotites enriched in ^{65}Cu. This is inconsistent with the observations of Savage et al. (2014) and Liu et al. (2015).

Liu et al. (2015) proposed that mantle melting generates no Cu isotope fractionation on the basis of the similar δ^{65}Cu of MORBs/OIBs and mantle peridotites devoid of metasomatism. However, the non-metasomatized peridotites investigated by Liu et al. (2015) display a significant range of δ^{65}Cu from −0.24 to 0.19‰, implying that other unidentified mantle processes had modified the Cu isotopic compositions of these peridotites. In addition, MORBs are generally the evolved products of primitive melts (Kelemen et al., 1995) and are modified by sulfide segregation during magma differentiation (O'Neill and Mavrogenes, 2002; Jenner et al., 2012; Patten et al., 2013). Sulfide segregation can elevate the δ^{65}Cu of the evolved melts (Huang et al., 2016a), and thus the Cu isotopic compositions of MORBs does not directly mirror those of primitive melts. Thus, it is inappropriate to directly compare δ^{65}Cu of MORBs/OIBs and peridotites to investigate Cu isotope fractionation during mantle melting. Savage et al. (2014) determined the Cu isotopic compositions of peridotites from Kilbourne Hole (Harvey et al., 2011, 2012) and found that the most melt-depleted harzburgites with the most unradiogenic $^{187}Os/^{188}Os$ have the lowest δ^{65}Cu (−0.40 to −0.20‰). Such low δ^{65}Cu might be attributed to isotope fractionation during partial melting under oxidized conditions, where redox reaction controls Cu isotope fractionation with ^{65}Cu preferentially entering the melts and thus enrichs ^{63}Cu in the residues. Alternatively, the low δ^{65}Cu of harzburgites could be caused by infiltration of oxidized fluids because such fluids would preferentially leach ^{65}Cu from the reactive solid rocks due to redox reactions (Mathur et al., 2005, 2012).

This interpretation is consistent with the petrological and geochemical results that the most melt-depleted harzburgite ($^{187}Os/^{188}Os$ ~0.1160, e.g., sample KH03-16) had been modified by CO_2- or H_2O-rich fluids as revealed by occurrence of small pockets and interstitial veins of SiO_2-rich glass and elevated bulk-rock $(La/Lu)_N$ (Harvey et al., 2011, 2012).

Copper commonly occurs in nature as monovalent and divalent (i.e., Cu^+ and Cu^{2+} compounds), which have distinct geochemistry and bonding strengths (e.g., Ehrlich et al., 2004). The valence of Cu in minerals and melts depends on the oxygen and sulfur fugacities because high oxygen fugacity (fO_2) can transform Cu^+ to Cu^{2+}, whereas high sulfur fugacity (fS_2) stabilizes the sulfide phase which contains Cu^+. For example, Liu et al. (2014c) experimentally showed that at the fO_2 of $\Delta FMQ \leq 1.2$ (log 10 unit deviations from the fayalite-magnetite-quartz (FMQ) buffer), Cu^+ is dominant in silicate melts, while Cu^{2+} is dominant at the fO_2 of $\Delta FMQ \geq 1.2$. Orogenic peridotite massifs typically record low fO_2 with ΔFMQ of −1.5 to −0.4 (Woodland et al., 1992) and hence Cu^+ should be the stable species in the melts. In addition, the prevalent presence of sulfides (e.g., Garuti et al., 1984; Wang et al., 2013) further suggests that partial melting of the BD and BM peridotites occurred at relatively low fO_2 and high fS_2, where Cu^+ was the dominant species in the melts and residues and controlled by the sulfide stability during mantle melting. Furthermore, Cu will be bonded to O in the melts and S in the residues, and thus a simple redox control is invalid. Experimental results have demonstrated that Cu solubility in silicate melts significantly increases with increasing fO_2 (e.g., Ripley et al., 2002; Liu et al., 2014c), suggesting that Cu^{2+} preferentially enters into the melts at high fO_2. As Cu^{2+} favors ^{65}Cu (e.g., Zhu et al., 2002; Ehrlich et al., 2004), mantle melting at high fO_2 will preferentially releases ^{65}Cu into the melts, leaving the residues enriched in ^{63}Cu. If so, $\delta^{65}Cu$ should be positively correlated with Al_2O_3 and Cu contents, which is opposite to the observations in this study. (Fig. 3A and B). Hence, redox reaction during mantle melting cannot explain the observed systematic variations of $\delta^{65}Cu$ with Al, Cu, S, Se, Te and Pd contents in the BD and BM lherzolites and harzburgites (Fig. 3).

About 0.30‰ Cu isotope fractionation occurs during partial melting of the DB and BM peridotites (Fig. 3). Such a fractionation is mainly controlled by equilibrium Cu isotope partitioning between sulfide and silicate, as revealed by the negative correlations between $\delta^{65}Cu$ and PGEs (e.g., Pd) and chalcophile elements (e.g., Cu, S, Se, and Te) (Fig. 3B–F). These relationships suggest that during partial melting of a sulfide-bearing mantle peridotite, sulfide breakdown would preferentially release ^{63}Cu into the melts. This is consistent with previous findings that sulfides are enriched in ^{63}Cu compared to co-existing silicates (Savage et al., 2015; Huang et al., 2016a). As interstitial sulfides in mantle rocks have higher $^{187}Os/^{188}Os$ and Pd/Ir relative to inclusion sulfides (Alard et al., 2000; Harvey et al., 2011; Burton et al., 2012), the negative correlations of $\delta^{65}Cu$ with $^{187}Os/^{188}Os$ and Pd/Ir (Fig. 4) further indicate that the preferential removal of interstitial sulfides is the major process causing significant Cu isotope fractionation observed in the BD and BM peridotites. Another implication of these relationships (Fig. 4) is that the average $\delta^{65}Cu$ of interstitial sulfides is higher than that of inclusion sulfides.

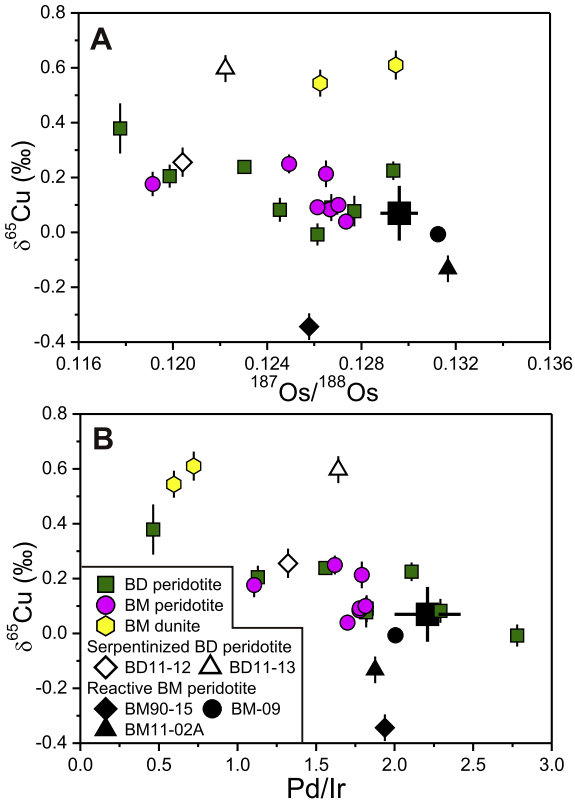

Fig. 4. $\delta^{65}Cu$ versus $^{187}Os/^{188}Os$ (A) and Pd/Ir (B) in Baldissero and Balmuccia peridotites. Black squares denote the primitive mantle (Becker et al., 2006; Savage et al., 2015).

Assuming variable Cu isotope fractionation factors between melts and sulfide-bearing peridotites ($\alpha_{melt\text{-}peridotite}$), the effect of melt extraction on Cu elemental and isotopic compositions of the residual peridotites was simulated (Fig. 5). A near-fractional melting model described in detail by Lee et al. (2012) was used to calculate Cu contents of aggregated melts as a function of bulk $^{peridotite/melt}D_{Cu}$ and melting degrees. In this model, the peridotite residues keep equilibrium with the instantaneous melts. At small increments (1%), equilibrium melts were removed and the compositions of the peridotite residues were updated accordingly. The initial mineralogy of 62% olivine, 20% orthopyroxene, 17% clinopyroxene, and 1% spinel are assumed (Lee et al., 2012). An initial bulk-rock S content in a fertile peridotite source of 200 ppm (Palme and O'Neill, 2014) and the average S content in the sulfide phase of about 363,600 ppm (e.g., Cu-Ni-sulfide) are assumed (Lee et al., 2012). This corresponds to 0.0556% sulfide phase in bulk rock and is also consistent with the petrological observations that pentlandite and subordinate chalcopyrite are the major base metal sulfides (>95% by volume) in the BD and BM peridotites (Wang et al., 2013). Copper contents of peridotite residues ($C_{residue}$)

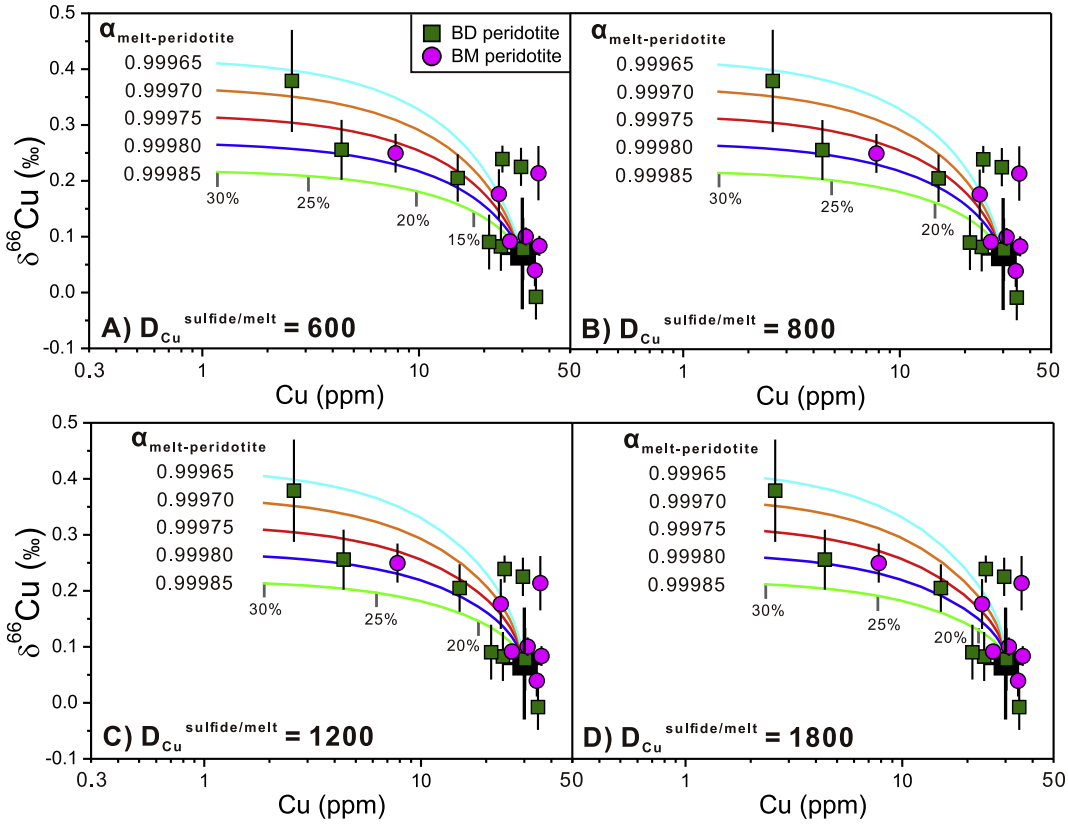

Fig. 5. $\delta^{65}Cu$ versus Cu in Baldissero and Balmuccia peridotites compared with modelling results with variable $\alpha_{melt\text{-}peridotite}$ at given ${}^{sulfide/melt}D_{Cu}$ of 600 (A), 800 (B), 1200 (C), and 1800 (D). The modelling curves denote Cu isotope fractionation during mantle partial melting assuming variable Cu isotope fractionation factors between melt and sulfide-bearing peridotite (i.e., $\alpha_{melt\text{-}peridotite}$) at conditions of variable Cu partition coefficients between sulfide and silicate melts (i.e., ${}^{sulfide/melt}D_{Cu}$) (See text and Supplementary materials for details). The ${}^{sulfide/melt}D_{Cu}$ covers the whole range of experimentally-determined values (e.g., Gaetani and Grove, 1997; Ripley et al., 2002; Mungall and Brenan, 2014). The correlation between $\delta^{65}Cu$ and Cu contents of the BD and BM peridotites can be explained by equilibrium fractionation with a $\alpha_{melt\text{-}peridotite}$ of 0.99965–0.99980, irrespective of the spread of ${}^{sulfide/melt}D_{Cu}$. For clarity, two dunites, a serpentinized lherzolite (BD11-13) and three BM lherzolites (BM90-15, BM-09, and BM11-02A) modified by local sulfide melt percolation are not included in this plot. The numbers below green curves are degrees of partial melting. Black square denotes the primitive mantle (Savage et al., 2015; Wang and Becker, 2015a). (For interpretation of the references to colour in this figure legend, the reader is referred to the web version of this article.)

and primitive melts (C_{melt}) at different degrees of mantle melting were calculated using the Program-Chalcophile Worksheet provided by Lee et al. (2012). We changed ${}^{sulfide/melt}D_{Cu}$ of 600, 800, 1200, and 1800 in our calculations to be consistent with the plausible range of experimentally-determined ${}^{sulfide/melt}D_{Cu}$ (600–1800, e.g., Gaetani and Grove, 1997; Ripley et al., 2002; Mungall and Brenan, 2014).

The isotope mass balance method in Craddock et al. (2013) was used here for Cu isotopes. The equation for calculating $\delta^{65}Cu_{residue}$ of peridotite residues is:

$$\delta^{65}Cu_{residue} = \delta^{65}Cu_0 - [1 - C_{residue} \times (1 - F)/C_0] \times 10^3 \ln\alpha_{melt\text{-}peridotite} \quad (1)$$

where C_0 and $\delta^{65}Cu_0$ is the Cu elemental and isotopic compositions of the mantle source (30 ppm, Wang and Becker, 2015a; 0.07‰, Savage et al., 2015), and $C_{residue}$ is the Cu contents of the peridotite residues at given degrees of melting (F). A more detailed description of the modelling processes can be found in *Supplementary materials*. The modelling variations of Cu contents and $\delta^{65}Cu$ in the residual peridotites at different degrees of melting are depicted in Fig. 5. The results show that the correlation between $\delta^{65}Cu$ and Cu contents of the BD and BM peridotites can be explained by equilibrium fractionation with a $\alpha_{melt\text{-}peridotite}$ of 0.99965 to 0.99980, regardless of the spread of ${}^{sulfide/melt}D_{Cu}$. These apparent $\alpha_{melt\text{-}peridotite}$ imply that if sulfide is an accessory phase in mantle peridotites during partial melting, $10^3\ln\alpha_{melt\text{-}peridotite} = -0.20$ to -0.35‰.

5.3. Copper isotope fractionation during melt percolation in the mantle

5.3.1. Sulfide melt percolation in peridotites

The spinel peridotite BM11-02A most likely records local mobilization of sulfide melts, as indicated by the high S (349 ppm) and Se (143 ppm) contents (Fig. 2B–E) as well as abundant interstitial sulfides (Wang et al., 2013). Because sample BM11-02A has similar Te and PGEs (e.g., Pd)

contents to those of other lherzolites (Fig. 2D and J), the sulfide melts must have been enriched in S and Se but more depleted in Te and PGEs. This behavior is different from what would be expected from basaltic melts near sulfide saturation (Wang et al., 2013). The light Cu isotopic composition of sample BM11-02A (Fig. 3) provide an independent evidence for the local addition of sulfide melts that are enriched in ^{63}Cu. In particular, addition of sulfide melts results in significant elevation of chalcophile element (e.g., Cu, S, Se, and Te) contents and decrease of δ^{65}Cu values in lherzolites BM11-02A and BM-09 (Fig. 3B–E), being opposite to the partial melting trend. This possibly indicates that equilibrium Cu isotope fractionation not only occurs during partial melting but also occurs between lherzolites BM11-02A and BM-09 and the percolated sulfide melts. Alternatively, the relatively high Cu contents and low δ^{65}Cu of BM11-02A and BM-09 (Fig. 3B) might be caused by kinetic isotope fractionation during sulfide melt percolation with a preferential diffusion of ^{63}Cu from the Cu-rich melts to peridotites. The spinel lherzolite BM90-15 has much higher Te contents (20.5 ppb) relative to, but Se contents similar to other lherzolites (Fig. 2D and E). Such anomalies might result from localized redistribution processes during cooling and/or a late-stage melt/fluid transport (e.g., Alard et al., 2011), which might have altered the Cu isotopic composition of lherzolite BM90-15, resulting in a marked deviation from the trend defined by other samples (Fig. 3B, D–F).

5.3.2. Silicate melt percolation in replacive dunites

Replacive dunites from the Oman and Troodos Ophiolites, formed during melt-peridotite interactions at high melt/rock ratios, represent conduits for focused melt flow (Kelemen et al., 1995). Dunites in the Balmuccia massif are also of replacive origin and formed later than lherzolites, as evidenced by the occurrence of relict websterite lenses in spinel-bearing dunites (Mazzucchelli et al., 2009) and gradual dissolution of pyroxenes from harzburgite into dunite at their boundary (Rivalenti et al., 1995; Wang et al., 2013). Petrological, elemental and Sr-Nd-Os isotopic evidence suggested that these highly refractory dunites have formed by focused percolation of deep-seated, S-undersaturated silicate melts after partial melting of lherzolites before their emplacement into crustal levels (Mazzucchelli et al., 2009; Wang et al., 2013; Wang and Becker, 2015b).

The coupled decrease of incompatible PGEs and S, Se, and Te as well as low Pd/Ir ratios (Figs. 2C–E, 4B) in dunites can be explained by preferential dissolution of interstitial sulfides during S-undersaturated melt-lherzolite interactions (Wang et al., 2013). The same process has been invoked to explain the variable Os contents (383–16 ppb) and highly fractionated ^{187}Os/^{188}Os ratios (0.129–0.140) of troctolites from the crust-mantle transition zone in the Indian Ocean (Sanfilippo et al., 2016). The variable and relatively high contents of compatible PGEs (e.g., Ir, Ru, Rh) but low contents of S, Se, Te, and incompatible PGEs in dunites (Wang et al., 2013) imply precipitation of Ir-Ru-Rh-rich metal alloys at high melt/rock ratios (e.g., Finnigan et al., 2008). Such metal alloys only precipitate from S-underasturated melts (Brenan and Andrews, 2001), which in turn supports S-undersaturated conditions during the formation of the BM replacive dunites. This is in agreement with the idea that the BM dunites formed in the mantle of the spinel stability field (Mazzucchelli et al., 2009), where the percolated melts have high sulfide capacity and thus are S-undersaturated (O'Neill and Mavrogenes, 2002). It is well known that S-undersaturated melt percolation cannot add radiogenic Os into mantle rocks (Ackerman et al., 2009; Liu et al., 2011). This can explain the similar Os isotopic compositions of the BM dunites and lherzolites (Fig. 4A) (Wang et al., 2013). In addition, the BM dunites, lherzolites and pyroxenite veins have similar Sr-Nd isotopic compositions (Voshage et al., 1988; Obermiller, 1994; Mazzucchelli et al., 2009), further suggesting that the S-undersaturated silicate melts were derived internally (i.e., a closed system).

Two dunites analyzed in this study display extremely heavy Cu isotopic compositions, with δ^{65}Cu of 0.544‰ and 0.610‰ (Figs. 3 and 4). Such high δ^{65}Cu cannot be attributed to chemical diffusion-driven kinetic isotope fractionation during melt percolation of the BM lherzolites. Deep-seated, mantle-derived mafic melts (e.g., 60–120 ppm in basaltic melts, Lee et al., 2012) have higher Cu contents relative to the BM lherzolites ($\leq$35 ppm, Table 1). As lighter isotopes generally diffuse faster than heavier ones (Richter et al., 2003), diffusion of Cu from a Cu-rich melt to lherzolites during melt percolation should cause an elevation of Cu contents and an enrichment of ^{63}Cu in the BM dunites (reaction products). This is inconsistent with their relatively low Cu contents and high δ^{65}Cu (Figs. 3 and 4). As discussed above, dunites had experienced dissolution of sulfides and precipitation of Ir-Ru-Rh-rich alloys during S-undersaturated melt percolation of their parental lherzolites. Ir-Ru-Rh-rich alloy grains in mantle peridotites contain no Cu (e.g., Walker et al., 2005) and thus should have no effect on the δ^{65}Cu of the BM dunites. Previous studies have shown that sulfide is enriched in ^{63}Cu compared to co-existing silicates (Savage et al., 2015; Huang et al., 2016a). Thus, we interpret the high δ^{65}Cu of the BM dunites as a result of preferential dissolution of interstitial sulfides in parental rocks (i.e., lherzolites) during S-undersaturated melt percolation. This process preferentially releases ^{63}Cu into the reactive S-undersaturated melts, resulting in an enrichment of ^{65}Cu in residual rocks (i.e., dunites).

5.4. Implications

5.4.1. Controls on Cu isotopic heterogeneity of the upper mantle

Copper isotopic measurements of orogenic and xenolithic peridotites have shown that the upper mantle has highly variable δ^{65}Cu from −0.64 to 1.82‰ (Savage et al., 2014; Liu et al., 2015; this study). Such a Cu isotopic heterogeneity has been interpreted to result from mantle metasomatism by fluids sourced from subducted hydrothermally altered oceanic lithosphere (Savage et al., 2014; Liu et al., 2015). This interpretation assumed no Cu isotope fractionation during mantle processes. However, our study

shows that Cu isotopes can also fractionate significantly during partial melting and melt percolation in the mantle.

Partial melting can result in Cu depletion in the residual peridotites due to its moderate incompatibility (e.g., Lee et al., 2012; Liu et al., 2014c) and will lead to ca. 0.30‰ Cu isotope fractionation (Figs. 5 and 6). Percolation of S-undersaturated silicate melts can cause a significant elevation of δ^{65}Cu (up to ca. 0.61‰) and variable Cu contents of peridotites due to isotopically light sulfide dissolution (Fig. 6). In the study of Liu et al. (2015), samples FS-50 and FS-64 have relatively high δ^{65}Cu, which may be due to Fe-rich and presumable S-undersaturated silicate melt percolation as revealed by the low Fo (molar Mg/(Mg + Fe)) of olivine and bulk-rock Pt enrichments (Liu et al., 2011). High Cu contents and low δ^{65}Cu in some peridotites can be explained by reaction of peridotites with isotopically light sulfide melts (Fig. 6). Alternatively, kinetic Cu isotope fractionation induced by chemical diffusion is likely to occur during sulfide melt-peridotite interactions. Diffusion of Cu from a Cu-rich melt to a host peridotite in the course of melt percolation could also produce combined high Cu contents and low δ^{65}Cu (Fig. 6). Thus, our study together with the previously-published data demonstrate that partial melting and percolation of different types of melts influence the Cu isotopic heterogeneity of the upper mantle.

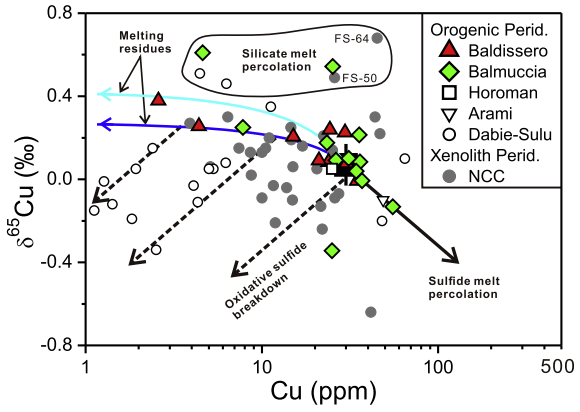

Fig. 6. Available δ^{65}Cu versus Cu of orogenic and xenolith peridotites reported in previous and present studies. Also shown are processes described in this study, which influence Cu isotopic compositions of peridotites. Partial melting (blue and cyan curves with arrows) results in Cu depletion and ^{65}Cu enrichment in the residual peridotites, while oxidative sulfide breakdown (dashed line with arrow) can further lead to Cu depletion but ^{63}Cu enrichment. Silicate melt percolation (circle field) produces variable Cu contents and high δ^{65}Cu, while sulfide melt percolation (bold black line with arrow) enriches peridotites in Cu and ^{63}Cu. For clarity, this plot only depicts the modelling variations of δ^{65}Cu and Cu contents in residual peridotites during partial melting assuming a maximum $\alpha_{\text{melt-peridotite}}$ of 0.99980 (blue curve) and a minimum $\alpha_{\text{melt-peridotite}}$ of 0.99965 (cyan curve) at a given $^{\text{sulfide/melt}}D_{Cu} = 600$ (the same as in Fig. 5A). Data sources for Orogenic Peridotite (Perid.): Baldissero and Balmuccia (this study), Horoman (Ikehata and Hirata, 2012), and Arami and Dabie-Sulu (Liu et al., 2015). Data for Xenolith Peridotite from North China Craton (NCC) are from Liu et al. (2015). Black square denotes the primitive mantle (Savage et al., 2015; Wang and Becker, 2015a). (For interpretation of the references to colour in this figure legend, the reader is referred to the web version of this article.)

It is noted that most peridotites compiled from the literature have lower Cu contents and lighter Cu isotopic compositions relative to the primitive mantle and the trend defined by the BD and BM peridotites (Fig. 6). These features can be explained by a two-stage process, i.e., partial melting and subsequent mantle metasomatism by fluids sourced from the subducted slabs. Partial melting results in the Cu depletion and moderate ^{65}Cu enrichments in the residual peridotites. It is known that slab-derived fluids have high fO_2 above the sulfide-sulfur oxide buffer (Sun et al., 2007). Addition of such oxidized fluids to the peridotites could result in oxidative sulfide breakdown, which is common during mantle metasomatism by slab-derived oxidized components, as revealed by studies of PGEs and Os isotopes (e.g., Lorand et al., 1999; Liu et al., 2011). As ^{65}Cu is preferentially leached into the fluid phases during sulfide redox reactions (e.g., Mathur et al., 2005, 2012), this process will shift the residual peridotites to lighter Cu isotopic compositions and lower Cu contents.

5.4.2. Controls on Cu isotopic systematics of mantle-derived magmas

In this section, we will investigate the controls on the Cu isotopic systematics of mantle-derived magmas (including MORBs and komatiites) based on our observation that mantle partial melting can result in significant Cu isotope fractionation. We do not take OIBs into account because their mantle sources could incorporate variable amounts of recycled ancient oceanic crust and sediments of different types (e.g., Hofmann, 1997; Stracke et al., 2003), which could overprint the Cu isotopic variations induced by partial melting. We have calculated the $\delta^{65}Cu_{melt}$ of primitive mantle-derived melts generated by variable degrees of mantle melting using the Eq. (2):

$$\delta^{65}Cu_{melt} = \delta^{65}Cu_0 + (1 - C_{melt} \times F/C_0) \times 10^3 \ln\alpha_{melt\text{-}peridotite} \quad (2)$$

where C_{melt} is the Cu contents of primitive melts at different degrees of melting (F) and is calculated using the Program-Chalcophile Worksheet provided by Lee et al. (2012), and the other parameters are the same as in Eq. (1). For clarity, we only calculated C_{melt} assuming $^{\text{sulfide/melt}}D_{Cu} = 600$ and 1800 (experimentally-determined minimum and maximum values, e.g., Gaetani and Grove, 1997; Ripley et al., 2002; Mungall and Brenan, 2014), and we only used the maximum and minimum $\alpha_{\text{melt-peridotite}}$ (0.99980 and 0.99965, respectively) estimated in this study. The whole procedures in detail can be found in *Supplementary Materials*, and the modelling results are shown in Fig. 7.

It has been widely accepted that MORBs are formed by 5–20% partial melting of the upper mantle (e.g., Hamlyn et al., 1985; Klein and Langmuir, 1987). Previous studies have shown that MORBs have δ^{65}Cu from 0 to 0.14‰ (Liu et al., 2015; Savage et al., 2015), heavier than those of primitive melts generated by 5–20% degrees of mantle melting (−0.26‰ to 0.00‰, Fig. 7). This offset can be explained by segregation of isotopically light sulfide during MORB magma differentiation (Fig. 7). Mid-ocean ridge

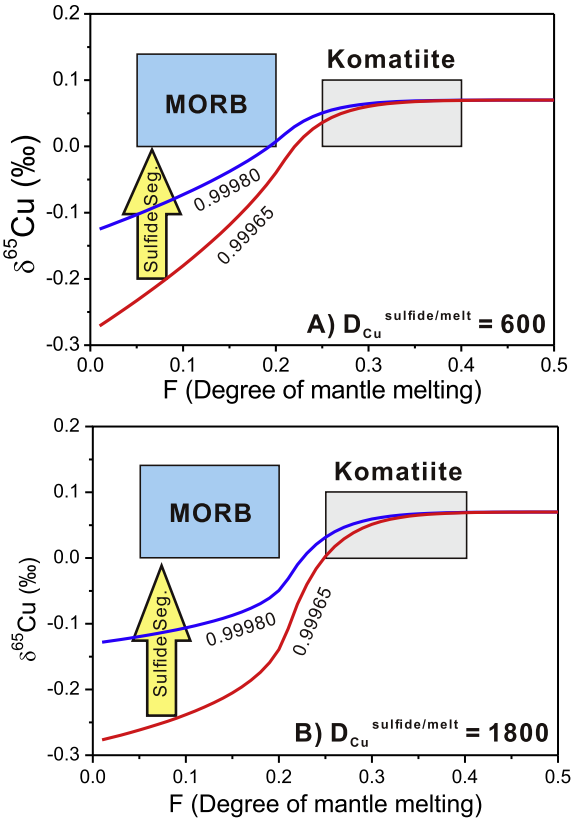

Fig. 7. Variations of δ^{65}Cu in primitive peridotite-derived melts with degrees of mantle melting (F). The δ^{65}Cu of primitive melts were modelled assuming a maximum $\alpha_{melt\text{-}peridotite}$ of 0.99980 (blue curve) and a minimum $\alpha_{melt\text{-}peridotite}$ of 0.99965 (red curve) at a minimum $^{sulfide/melt}D_{Cu}$ of 600 (A) and a maximum $^{sulfide/melt}D_{Cu}$ of 1800 (B) (See text and Supplementary materials for details). The δ^{65}Cu of MORBs are higher than those of the primitive melts generated by 5–20% degrees of mantle melting. This discrepancy can be explained by a small fraction of isotopically light sulfide segregation (Seg.) (light yellow arrows). High degrees (>25‰) of melting extracts nearly all Cu in the mantle source, and thus komatiites, formed by about 25–45% degrees of partial melting (Sossi et al., 2016b), have similar Cu isotopic compositions to the primitive mantle. Global MORBs (δ^{65}Cu = 0–0.14‰, N = 24, Savage et al., 2015; Liu et al., 2015) and komatiites (δ^{65}Cu = 0–0.11‰, N = 14, Savage et al., 2015). (For interpretation of the references to colour in this figure legend, the reader is referred to the web version of this article.)

basalts are commonly saturated in S before eruption as revealed by the presence of sulfide droplets enclosed in fresh MORB glasses (Jenner et al., 2012; Patten et al., 2013) and by experimental studies of S solubility in silicate melts (O'Neill and Mavrogenes, 2002). The large variations of the PGE and Te abundances in terrestrial basalts have been interpreted to reflect variable extents of sulfide segregation during their evolution (e.g., Patten et al., 2013; Lissner et al., 2014). Based on the correlations of S and MgO in MORB glasses from the Atlantic, Indian and Pacific Ridges (Jenner and O'Neill, 2012), the calculated mass fraction of segregated sulfide is from ~0 to 0.23‰ (Kiseeva and Wood, 2015).

Sulfide can be exhausted when the degree of a fertile mantle melting is more than 20–25% (Hamlyn et al., 1985; Lee et al., 2012). Considering that Cu is almost exclusively sulfide-controlled, nearly all Cu in the mantle source will be partitioned into the melts at high degrees of melting. Our modelling results show that primitive melts generated by 25–50% degrees of partial melting have relatively homogeneous δ^{65}Cu (0.00–0.07‰) (Fig. 7), identical to that of the primitive mantle source (0.07 ± 0.10‰, Savage et al., 2015). Thus, it is not surprising that komatiites (0.059 ± 0.064‰, 2SD, n = 14, Savage et al., 2015), formed by high degrees of melting (~25 to 40%, Sossi et al., 2016b), have identical δ^{65}Cu with the primitive mantle (Fig. 7).

6. CONCLUSIONS

Based on high-precision Cu isotopic measurements of the Baldissero and Balmuccia massif peridotites from the IVZ (Northern Italy), the following conclusions can be drawn:

(1) Fresh lherzolites and harzburgites show variable δ^{65}Cu values (−0.133 to 0.379‰) that display negative correlations with Al_2O_3, Cu, S, Se, Te and Pd contents, indicating Cu isotope fractionation during partial melting and sulfide melt percolation. The removal of sulfides enriched in ^{63}Cu during partial melting results in the elevation of δ^{65}Cu in the residual peridotites, whereas sulfide melt percolation has an opposite effect. If sulfide exists in the peridotite during partial melting, $\alpha_{melt\text{-}peridotite}$ is 0.99980–0.99965 as estimated from the correlation between δ^{65}Cu and Cu contents of the Baldissero and Balmuccia sulfide-bearing peridotite.

(2) Replacive dunites have relatively high δ^{65}Cu (0.544–0.610‰) that might result from dissolution of isotopically light sulfides during the focused flow of S-undersaturated melts and re-equilibration of their parental lherzolites.

(3) Copper isotopic heterogeneity of the upper mantle could be related to partial melting, percolation of deep-seated melts with different compositions, and oxidative sulfide breakdown due to mantle metasomatism by slab-derived oxidized fluids.

(4) Copper isotopic compositions of MORBs are influenced by partial melting and sulfide segregation during magma evolution. The similarity of δ^{65}Cu between komatiites and the primitive mantle is best explained by the fact that high degrees (>25%) of partial melting extracts nearly all Cu in the mantle source.

ACKNOWLEDGEMENT

This study is financially supported by grants from the DREAM Project of MOST China (NO. 2016YFC0600404) and the National Natural Science Foundation of China (NOs. 41573018, 41325011). Thanks are due to W.-Y, Li for polishing English and discussions on early version of this manuscript. We gratefully acknowledge

Alessio Sanfilippo and one anonymous reviewer for thorough and constructive reviews, and Andreas Stracke for comments and the editorial handling, which greatly improved this manuscript.

APPENDIX A. SUPPLEMENTARY MATERIAL

Supplementary data associated with this article can be found, in the online version, at http://dx.doi.org/10.1016/j.gca.2017.05.007.

REFERENCES

Ackerman L., Walker R. J., Puchtel I. S., Pitcher L., Jelínek E. and Strnad L. (2009) Effects of melt percolation on highly siderophile elements and Os isotopes in subcontinental lithospheric mantle: a study of the upper mantle profile beneath Central Europe. *Geochem. Cosmochim. Acta* **73**, 2400–2414.

Alard O., Griffin W. L., Lorand J. P., Jackson S. E. and O'Reilly S. Y. (2000) Non-chondritic distribution of the highly siderophile elements in mantle sulphides. *Nature* **407**, 891–894.

Alard O., Lorand J.-P., Reisberg L., Bodinier J.-L., Dautria J.-M. and O'Reilly S. Y. (2011) Volatile-rich metasomatism in Montferrier xenoliths (Southern France): implications for the abundances of chalcophile and highly siderophile elements in the subcontinental mantle. *J. Petrol.* **52**, 2009–2045.

Albarède F. (2004) The stable isotope geochemistry of copper and zinc. *Rev. Mineral. Geochem.* **55**, 409–427.

An Y., Huang J.-X., Griffin W. L., Liu C. and Huang F. (2017) Isotopic composition of Mg and Fe in garnet peridotites from the Kaapvaal and Siberian cratons. *Geochim. Cosmochim. Acta* **200**, 167–185.

Becker H., Horan M. F., Walker R. J., Gao S., Lorand J. P. and Rudnick R. L. (2006) Highly siderophile element composition of the Earth's primitive upper mantle: constraints from new data on peridotite massifs and xenoliths. *Geochim. Cosmochim. Acta* **70**, 4528–4550.

Bigalke M., Weyer S., Kobza J. and Wilcke W. (2010a) Stable Cu and Zn isotope ratios as tracers of sources and transport of Cu and Zn in contaminated soil. *Geochim. Cosmochim. Acta* **74**, 6801–6813.

Bigalke M., Weyer S. and Wilcke W. (2010b) Copper isotope fractionation during complexation with insolubilized humic acid. *Environ. Sci. Technol.* **44**, 5496–5502.

Bigalke M., Weyer S. and Wilcke W. (2011) Stable Cu isotope fractionation in soils during oxic weathering and podzolization. *Geochim. Cosmochim. Acta* **75**, 3119–3134.

Bodinier J. L. and Godard M. (2014) 3.4 – Orogenic, ophiolitic, and abyssal peridotites A2 – Holland, Heinrich D. In *Treatise on Geochemistry (Second Edition)* (ed. K. K. Turekian). Elsevier, Oxford, pp. 103–167.

Brenan J. M. and Andrews D. (2001) High-temperature stability of laurite and Ru-Os-Rh alloy and their role in PGE fractionation in mafic magmas. *Can. Mineral.* **39**, 341–360.

Burton K. W., Cenki-Tok B., Mokadem F., Harvey J., Gannoun A., Alard O. and Parkinson I. J. (2012) Unradiogenic lead in Earth/'s upper mantle. *Nat. Geosci.* **5**, 570–573.

Chapman J. B., Mason T. F. D., Weiss D. J., Coles B. J. and Wilkinson J. J. (2006) Chemical separation and isotopic variations of Cu and Zn from five geological reference materials. *Geostand. Geoanalyt. Res.* **30**, 5–16.

Craddock P. R., Warren J. M. and Dauphas N. (2013) Abyssal peridotites reveal the near-chondritic Fe isotopic composition of the Earth. *Earth Planet. Sci. Lett.* **365**, 63–76.

Dekov V. M., Rouxel O., Asael D., Hålenius U. and Munnik F. (2013) Native Cu from the oceanic crust: isotopic insights into native metal origin. *Chem. Geol.* **359**, 136–149.

Doucet L. S., Mattielli N., Ionov D. A., Debouge W. and Golovin A. V. (2016) Zn isotopic heterogeneity in the mantle: a melting control? *Earth Planet. Sci. Lett.* **451**, 232–240.

Ehrlich S., Butler I., Halicz L., Rickard D., Oldroyd A. and Matthews A. (2004) Experimental study of the copper isotope fractionation between aqueous Cu(II) and covellite, CuS. *Chem. Geol.* **209**, 259–269.

Fellows S. A. and Canil D. (2012) Experimental study of the partitioning of Cu during partial melting of Earth's mantle. *Earth Planet. Sci. Lett.* **337–338**, 133–143.

Finnigan C. S., Brenan J. M., Mungall J. E. and McDonough W. F. (2008) Experiments and models bearing on the role of chromite as a collector of platinum group minerals by local reduction. *J. Petrol.* **49**, 1647–1665.

Gaetani G. A. and Grove T. L. (1997) Partitioning of moderately siderophile elements among olivine, silicate melt, and sulfide melt: constraints on core formation in the Earth and Mars. *Geochim. Cosmochim. Acta* **61**, 1829–1846.

Garuti G., Gorgoni C. and Sighinolfi G. P. (1984) Sulfide mineralogy and chalcophile and siderophile element abundances in the Ivrea-Verbano mantle peridotites (Western Italian Alps). *Earth Planet. Sci. Lett.* **70**, 69–87.

Hamlyn P. R., Keays R. R., Cameron W. E., Crawford A. J. and Waldron H. M. (1985) Precious metals in magnesian low-Ti lavas: implications for metallogenesis and sulfur saturation in primary magmas. *Geochim. Cosmochim. Acta* **49**, 1797–1811.

Harvey J., Dale C. W., Gannoun A. and Burton K. W. (2011) Osmium mass balance in peridotite and the effects of mantle-derived sulphides on basalt petrogenesis. *Geochem. Cosmochim. Acta* **75**, 5574–5596.

Harvey J., Yoshikawa M., Hammond S. J. and Burton K. W. (2012) Deciphering the trace element characteristics in Kilbourne Hole peridotite xenoliths: melt-rock interaction and metasomatism beneath the Rio Grande Rift, SW USA. *J. Petrol.* **53**, 1709–1742.

Hartmann G. and Hans Wedepohl K. (1993) The composition of peridotite tectonites from the Ivrea Complex, northern Italy: residues from melt extraction. *Geochem. Cosmochim. Acta* **57**, 1761–1782.

Hofmann A. W. (1997) Mantle geochemistry: the message from oceanic volcanism. *Nature* **385**, 219–229.

Huang J., Liu S.-A., Wörner G., Yu H. M. and Xiao Y. L. (2016a) Copper isotope behavior during extreme magma differentiation and degassing: a case study on Laacher See phonolite tephra (East Eifel, Germany). *Contrib. Mineral. Petrol.* **171**, 1–16.

Huang J., Liu S.-A., Gao Y. J., Xiao Y. L. and Chen S. (2016b) Copper and zinc isotope systematics of altered oceanic crust at IODP Site 1256 in the eastern equatorial Pacific. *J. Geophys. Res.* **121**, 7086–7100.

Ikehata K. and Hirata T. (2012) Copper isotope characteristics of copper-rich minerals from the Horoman peridotite complex, Hokkaido, Northern Japan. *Econ. Geol.* **107**, 1489–1497.

Jenner F. E., Arculus R. J., Mavrogenes J. A., Dyriw N. J., Nebel O. and Hauri E. H. (2012) Chalcophile element systematics in volcanic glasses from the northwestern Lau Basin. *Geochem. Geoph. Geosyst.* **13**, Q06014.

Jenner F. E. and O'Neill H. S. C. (2012) Analysis of 60 elements in 616 ocean floor basaltic glasses. *Geochem., Geophys. Geosyst.* **13**, Q02005, http://doi:02010.01029/02011GC004009.

Kelemen P. B., Shimizu N. and Salters V. J. M. (1995) Extraction of mid-ocean-ridge basalt from the upwelling mantle by focused flow of melt in dunite channels. *Nature* **375**, 747–753.

Kiseeva E. S. and Wood B. J. (2015) The effects of composition and temperature on chalcophile and lithophile element partitioning into magmatic sulphides. *Earth Planet. Sci. Lett.* **424**, 280–294.

Klein E. M. and Langmuir C. H. (1987) Global correlations of ocean ridge basalt chemistry with axial depth and crustal thickness. *J. Geophys. Res.* **92**, 8089–8115.

Le Roux V., Dasgupta R. and Lee C.-T. A. (2015) Recommended mineral-melt partition coefficients for FRTEs (Cu), Ga, and Ge during mantle melting. *Amer. Mineral.* **100**, 2533–2544.

Lee C.-T. A., Luffi P., Chin E. J., Bouchet R., Dasgupta R., Morton D. M., Le Roux V., Yin Q.-Z. and Jin D. (2012) Copper systematics in arc magmas and implications for crust-mantle differentiation. *Science* **336**, 64–68.

Li W. Q., Jackson S. E., Pearson N. J., Alard O. and Chappell B. W. (2009) The Cu isotopic signature of granites from the Lachlan Fold Belt, SE Australia. *Chem. Geol.* **258**, 38–49.

Li W. Q., Jackson S. E., Pearson N. J. and Graham S. (2010) Copper isotopic zonation in the Northparkes porphyry Cu–Au deposit, SE Australia. *Geochim. Cosmochim. Acta* **74**, 4078–4096.

Lissner M., König S., Luguet A., le Roux P. J., Schuth S., Heuser A. and le Roex A. P. (2014) Selenium and tellurium systematics in MORBs from the southern Mid-Atlantic Ridge (47–50°S). *Geochem. Cosmochim. Acta* **144**, 379–402.

Liu J. G., Rudnick R. L., Walker R. J., Gao S., Wu F.-Y., Piccoli P. M., Yuan H. L., Xu W.-L. and Xu Y.-G. (2011) Mapping lithospheric boundaries using Os isotopes of mantle xenoliths: an example from the North China Craton. *Geochem. Cosmochim. Acta* **75**, 3881–3902.

Liu S.-A., Li D., Li S., Teng F.-Z., Ke S., He Y. and Lu Y. (2014a) High-precision copper and iron isotope analysis of igneous rock standards by MC-ICP-MS. *J. Anal. At. Spectrom.* **29**, 122–133.

Liu S.-A., Teng F.-Z., Li S., Wei G.-J., Ma J.-L. and Li D. (2014b) Copper and iron isotope fractionation during weathering and pedogenesis: insights from saprolite profiles. *Geochim. Cosmochim. Acta* **146**, 59–75.

Liu X. C., Xiong X. L., Audétat A., Li Y., Song M., Li L., Sun W. D. and Ding X. (2014c) Partitioning of copper between olivine, orthopyroxene, clinopyroxene, spinel, garnet and silicate melts at upper mantle conditions. *Geochim. Cosmochim. Acta* **125**, 1–22.

Liu S.-A., Huang J., Liu J. G., Wörner G., Yang W., Tang Y.-J., Chen Y., Tang L. M., Zheng J. P. and Li S. G. (2015) Copper isotopic composition of the silicate Earth. *Earth Planet. Sci. Lett.* **427**, 95–103.

Lorand J. P. (1989) Mineralogy and chemistry of Cu-Fe-Ni sulfides in orogenic-type spinel peridotite bodies from Ariege (Northeastern Pyrenees, France). *Contrib. Mineral. Petrol.* **103**, 335–345.

Lorand J.-P., Pattou L. and Gros M. (1999) Fractionation of platinum-group elements and gold in the upper mantle: a detailed study in pyrenean orogenic lherzolites. *J. Petrol.* **40**, 957–981.

Lorand J.-P. and Alard O. (2001) Platinum-group element abundances in the upper mantle: new constraints from in situ and whole-rock analyses of Massif Central xenoliths (France). *Geochem. Cosmochim. Acta* **65**, 2789–2806.

Luck J.-M., Othman D. B. and Albarède F. (2005) Zn and Cu isotopic variations in chondrites and iron meteorites: early solar nebula reservoirs and parent-body processes. *Geochim. Cosmochim. Acta* **69**, 5351–5363.

Luguet A., Alard O., Lorand J. P., Pearson N. J., Ryan C. and O'Reilly S. Y. (2001) Laser-ablation microprobe (LAM)-ICPMS unravels the highly siderophile element geochemistry of the oceanic mantle. *Earth Planet. Sci. Lett.* **189**, 285–294.

Luguet A., Lorand J.-P. and Seyler M. (2003) Sulfide petrology and highly siderophile element geochemistry of abyssal peridotites: a coupled study of samples from the Kane Fracture Zone (45° W 23°20N, MARK area, Atlantic Ocean). *Geochem. Cosmochim. Acta* **67**, 1553–1570.

Luguet A., Lorand J.-P., Alard O. and Cottin J.-Y. (2004) A multi-technique study of platinum group element systematic in some Ligurian ophiolitic peridotites, Italy. *Chem. Geol.* **208**, 175–194.

Mathur R., Ruiz J., Titley S., Liermann L., Buss H. and Brantley S. (2005) Cu isotopic fractionation in the supergene environment with and without bacteria. *Geochim. Cosmochim. Acta* **69**, 5233–5246.

Mathur R., Titley S., Barra F., Brantley S., Wilson M., Phillips A., Munizaga F., Maksaev V., Vervoort J. and Hart G. (2009) Exploration potential of Cu isotope fractionation in porphyry copper deposits. *J. Geochem. Expl.* **102**, 1–6.

Mathur R., Dendas M., Titley S. and Phillips A. (2010) Patterns in the copper isotope composition of minerals in porphyry copper deposits in Southwestern United States. *Econ. Geol.* **105**, 1457–1467.

Mathur R., Jin L., Prush V., Paul J., Ebersole C., Fornadel A., Williams J. Z. and Brantley S. (2012) Cu isotopes and concentrations during weathering of black shale of the Marcellus Formation, Huntingdon County, Pennsylvania (USA). *Chem. Geol.* **304–305**, 175–184.

Maréchal C. N., Télouk P. and Albarède F. (1999) Precise analysis of copper and zinc isotopic compositions by plasma-source mass spectrometry. *Chem. Geol.* **156**, 251–273.

Mazzucchelli M., Rivalenti G., Brunelli D., Zanetti A. and Boari E. (2009) Formation of highly refractory dunite by focused percolation of pyroxenite-derived melt in the Balmuccia peridotite massif (Italy). *J. Petrol.* **50**, 1205–1233.

Mazzucchelli M., Zanetti A., Rivalenti G., Vannucci R., Correia C. T. and Tassinari C. C. G. (2010) Age and geochemistry of mantle peridotites and diorite dykes from the Baldissero body: insights into the Paleozoic-Mesozoic evolution of the Southern Alps. *Lithos* **119**, 485–500.

Moeller K., Schoenberg R., Pedersen R.-B., Weiss D. and Dong S. (2012) Calibration of the new certified reference materials ERM-AE633 and ERM-AE647 for copper and IRMM-3702 for zinc isotope amount ratio determinations. *Geostand. Geoanalyt. Res.* **36**, 177–199.

Moynier F., Koeberl C., Beck P., Jourdan F. and Telouk P. (2010) Isotopic fractionation of Cu in tektites. *Geochim. Cosmochim. Acta* **74**, 799–807.

Moynier F., Vance D., Fujii T. and Savage P. (2017) The isotope geochemistry of zinc and copper. *Rev. Mineral. Geochem.* **82**, 543–600.

Mukasa S. B. and Shervais J. W. (1999) Growth of subcontinental lithosphere: evidence from repeated dike injections in the Balmuccia lherzolite massif, Italian Alps. *Lithos* **48**, 287–316.

Mungall J. E. and Brenan J. M. (2014) Partitioning of platinum-group elements and Au between sulfide liquid and basalt and the origins of mantle-crust fractionation of the chalcophile elements. *Geochim. Cosmochim. Acta* **125**, 265–289.

Obermiller W. A. (1994) *Chemical and Isotopic Variations in the Balmuccia, Baldissero and Finero Peridotite Massifs (Ivrea-Zone, Italy)* Ph.D. thesis. Johannes Gutenberg-Universitat Mainz, p. 191.

O'Neill H. S. C. and Mavrogenes J. A. (2002) The sulfide capacity and the sulfur content at sulfide saturation of silicate melts at 1400 °C and 1 bar. *J. Petrol.* **43**, 1049–1087.

Palme H. and O'Neill H. S. C. (2014) 3.1 – Cosmochemical estimates of mantle composition A2 – Holland, Heinrich D. In *Treatise on Geochemistry (Second Edition)* (ed. K. K. Turekian). Elsevier, Oxford, pp. 1–39.

Patten C., Barnes S.-J., Mathez E. A. and Jenner F. E. (2013) Partition coefficients of chalcophile elements between sulfide and silicate melts and the early crystallization history of sulfide liquid: LA-ICP-MS analysis of MORB sulfide droplets. *Chem. Geol.* **358**, 170–188.

Peressini G., Quick J. E., Sinigoi S., Hofmann A. W. and Fanning M. (2007) Duration of a large mafic intrusion and heat transfer in the lower crust: a SHRIMP U-Pb zircon study in the Ivrea-Verbano Zone (Western Alps, Italy). *J. Petrol.* **48**, 1185–1218.

Quick J. E., Sinigoi S., Peressini G., Demarchi G., Wooden J. L. and Sbisà A. (2009) Magmatic plumbing of a large Permian caldera exposed to a depth of 25 km. *Geology* **37**, 603–606.

Richter F. M., Davis A. M., DePaolo D. J. and Watson E. B. (2003) Isotope fractionation by chemical diffusion between molten basalt and rhyolite. *Geochim. Cosmochim. Acta* **67**, 3905–3923.

Ripley E. M., Brophy J. G. and Li C. (2002) Copper solubility in a basaltic melt and sulfide liquid/silicate melt partition coefficients of Cu and Fe. *Geochim. Cosmochim. Acta* **66**, 2791–2800.

Rivalenti G., Mazzucchelli M., Vannucci R., Hofmann A. W., Ottolini L., Bottazzi P. and Obermiller W. (1995) The relationship between websterite and peridotite in the Balmuccia peridotite massif (NW Italy) as revealed by trace element variations in clinopyroxene. *Contrib. Mineral. Petrol.* **121**, 275–288.

Sanfilippo A., Morishita T. and Senda R. (2016) Rhenium-osmium isotope fractionation at the oceanic crust-mantle boundary. *Geology* **44**, 167–170.

Shervais J. W. and Mukasa S. B. (1991) The Balmuccia orogenic lherzolite massif, Italy. *J. Spec.* **2**, 155–174.

Savage P. S., Harvey J. and Moynier F. (2014) Copper isotope heterogeneity in the lithospheric mantle. Goldschmidt 2014 Conference Abstracts, 2192.

Savage P. S., Moynier F., Chen H., Shofner G., Siebert J., Badro J. and Puchtel I. S. (2015) Copper isotope evidence for large-scale sulphide fractionation during Earth's differentiation. *Geochem. Perspect. Lett.* **1**, 53–64.

Shields W. R., Murphy T. J. and Garner E. L. (1964) Absolute isotopic abundance ratio and the atomic weight of a reference sample of copper. *J. Res. NBS* **68A**, 589–592.

Sossi P. A., Halverson G. P., Nebel O. and Eggins S. M. (2015) Combined separation of Cu, Fe and Zn from rock matrices and improved analytical protocols for stable isotope determination. *Geostand. Geoanalyt. Res.* **39**, 129–149.

Sossi P. A., Nebel O. and Foden J. (2016a) Iron isotope systematics in planetary reservoirs. *Earth Planet. Sci. Lett.* **452**, 295–308.

Sossi P. A., Eggins S. M., Nesbitt R. W., Nebel O., Hergt J. M., Campbell I. H., O'Neill H. S. C., Van Kranendonk M. and Davies D. R. (2016b) Petrogenesis and geochemistry of Archean komatiites. *J. Petrol.* **57**, 147–184.

Stracke A., Bizimis M. and Salters V. J. M. (2003) Recycling oceanic crust: quantitative constraints. *Geochem. Geophys. Geosyst.* **4**, Q8003. http://dx.doi.org/10.1029/2001GC000223.

Sun X., Tang Q., Sun W., Xu L., Zhai W., Liang J., Liang Y., Shen K., Zhang Z. and Zhou B. (2007) Monazite, iron oxide and barite exsolutions in apatite aggregates from CCSD drillhole eclogites and their geological implications. *Geochim. Cosmochim. Acta* **71**, 2896–2905.

Tomascak P. B., Tera F., Helz R. T. and Walker R. J. (1999) The absence of lithium isotope fractionation during basalt differentiation: new measurements by multicollector sector ICP-MS. *Geochim. Cosmochim. Acta* **63**, 907–910.

Voshage H., Sinigoi S., Mazzucchelli M., Demarchi G., Rivalenti G. and Hofmann A. W. (1988) Isotopic constraints on the origin of ultramafic and mafic dikes in the Balmuccia peridotite (Ivrea Zone). *Contrib. Mineral. Petrol.* **100**, 261–267.

Walker R. J., Brandon A. D., Bird J. M., Piccoli P. M., McDonough W. F. and Ash R. D. (2005) ^{187}Os–^{186}Os systematics of Os–Ir–Ru alloy grains from southwestern Oregon. *Earth Planet. Sci. Lett.* **230**, 211–226.

Walter M. J. (1998) Melting of garnet peridotite and the origin of komatiite and depleted lithosphere. *J. Petrol.* **39**, 29–60.

Wang K.-L., O'Reilly S. Y., Griffin W. L., Pearson N. J. and Zhang M. (2009) Sulfides in mantle peridotites from Penghu Islands, Taiwan: melt percolation, PGE fractionation, and the lithospheric evolution of the South China block. *Geochem. Cosmochim. Acta* **73**, 4531–4557.

Wang Z. C. and Becker H. (2013) Ratios of S, Se and Te in the silicate Earth require a volatile-rich late veneer. *Nature* **499**, 328–331.

Wang Z. C., Becker H. and Gawronski T. (2013) Partial re-equilibration of highly siderophile elements and the chalcogens in the mantle: a case study on the Baldissero and Balmuccia peridotite massifs (Ivrea Zone, Italian Alps). *Geochem. Cosmochim. Acta* **108**, 21–44.

Wang Z. C. and Becker H. (2015a) Abundances of Ag and Cu in mantle peridotites and the implications for the behavior of chalcophile elements in the mantle. *Geochem. Cosmochim. Acta* **160**, 209–226.

Wang Z. C. and Becker H. (2015b) Fractionation of highly siderophile and chalcogen elements during magma transport in the mantle: constraints from pyroxenites of the Balmuccia peridotite massif. *Geochem. Cosmochim. Acta* **159**, 244–263.

Weyer S. and Ionov D. A. (2007) Partial melting and melt percolation in the mantle: the message from Fe isotopes. *Earth Planet. Sci. Lett.* **259**, 119–133.

Woodland A. B., Kornprobst J. and Wood B. J. (1992) Oxygen thermobarometry of orogenic lherzolite massifs. *J. Petrol.* **33**, 203–230.

Xiao Y., Teng F.-Z., Zhang H.-F. and Yang W. (2013) Large magnesium isotope fractionation in peridotite xenoliths from eastern North China craton: Product of melt–rock interaction. *Geochim. Cosmochim. Acta* **115**, 241–261.

Zhao X.-M., Zhang H.-F., Zhu X.-K., Zhu B. and Cao H.-H. (2015) Effects of melt percolation on iron isotopic variation in peridotites from Yangyuan, North China Craton. *Chem. Geol.* **401**, 96–110.

Zhu X. K., Guo Y., Williams R. J. P., O'Nions R. K., Matthews A., Belshaw N. S., Canters G. W., de Waal E. C., Weser U., Burgess B. K. and Salvato B. (2002) Mass fractionation processes of transition metal isotopes. *Earth Planet. Sci. Lett.* **200**, 47–62.

Associate Editor: Andreas Stracke